

# Transport and tumbling of polymers in viscoelastic shear flow

Sadhana Singh,<sup>1</sup> R. K. Singh,<sup>1,2,\*</sup> and Sanjay Kumar<sup>1</sup>

<sup>1</sup>*Department of Physics, Banaras Hindu University, Varanasi-221005*

<sup>2</sup>*Department of Physics, Indian Institute of Technology, Bombay, Powai, Mumbai-400076*

Polymers in shear flow are ubiquitous and we study their motion in a viscoelastic fluid under shear. Employing dumbbells as representative, we find that the center of mass motion follows:  $\langle x_c^2(t) \rangle \sim \dot{\gamma}^2 t^{\alpha+2}$ ,  $0 < \alpha < 1$ , generalizing the earlier result:  $\langle x_c^2(t) \rangle \sim \dot{\gamma}^2 t^3$  ( $\alpha = 1$ ). Motion of the relative coordinate, on the other hand, is quite intriguing in that  $\langle x_r^2(t) \rangle \sim t^\beta$  with  $\beta = 2(1 - \alpha)$  for small  $\alpha$ . This implies nonexistence of the steady state. We remedy this pathology by introducing a nonlinear spring with FENE-LJ interaction and study tumbling dynamics of the dumbbell. The overall effect of viscoelasticity is to slow down the dynamics in the experimentally observed ranges of the Weissenberg number. We numerically obtain the characteristic time of tumbling and show that small changes in  $\alpha$  result in large changes in tumbling times.

*Introduction:* Viscoelastic fluids under shear are ubiquitous, especially in biological systems, and aid in transport of biomolecules *in-vivo*. Viscoelasticity, as the name suggests, is the property of a material comprising of both viscous and elastic behavior [1]. Almost all materials with biological or engineering interests are viscoelastic to some degree [2]. The elastic component of the material tends to bring it back to its original configuration when put under stress [3]. As a result, motion in viscoelastic media is generally slower, *i.e.*- the mean square displacement  $\langle x^2(t) \rangle \sim t^\alpha$  [4], with  $0 < \alpha < 1$ , consequent of the anti-persistent correlations in successive displacements [5]. Viscoelastic subdiffusion frequently arises in motion in biological domains, *e.g.*- motion in crowded fluids [6], cytoplasm of living cells [7], locus of a chromosome in eukaryotes [8], etc.

Even though a useful representative of system dynamics, a single particle description is not fully appropriate when it comes to investigating systems with internal degrees of freedom, *e.g.*- polymers. In addition, polymers constitute the basic building blocks of the macromolecules like DNA and proteins. Hence, it becomes natural to investigate the dynamical aspects of a polymer in viscoelastic media. However, most of the polymer transport *in-vivo* takes place in viscoelastic fluids under shear, wherein they not only move but also tumble along, *i.e.*- an end-to-end rotation. The phenomena of polymer tumbling is well understood for the case of viscous shear flows [9, 10]. And arises when the relaxation time of the polymer is larger than the time-scale of flow deformation [11], with characteristic tumbling time varying sublinearly with the flow rate [12, 13]. However, a majority of studies involving tumbling do not cover the practically important case of shear flows arising in viscoelastic media, *e.g.*- polymer plastics and most of the biological materials [14].

These observations raise an interesting question: what are the dynamical characteristics of a polymer in a viscoelastic fluid under shear? This is a question of immense

practical significance, which we answer in the present work employing a dumbbell which is the simplest form of a polymer. For the two masses connected by a harmonic spring, we show both analytically and numerically that the separation grows without bounds. This implies towards the nonexistence of steady state and essentially means that tumbling cannot be addressed using a linear system. We remedy this pathology by introducing a finitely extensible nonlinear elastic spring with repulsive part of the Lennard-Jones interaction (FENE-LJ) [15, 16]. Thus, allowing us to address tumbling.

*Generalized Langevin equation in shear flows:* The generalized Langevin equation (GLE) [17] describing the motion of a dumbbell in a viscoelastic material under shear reads:

$$\int_0^t dt' \eta(t-t') (\dot{\mathbf{r}}_i - \dot{\gamma} y_i \mathbf{i})(t') = -\nabla_i V(|\mathbf{r}_i - \mathbf{r}_j|) + \xi_i(t), \quad (1)$$

where  $\mathbf{r}_i \equiv (x_i, y_i, z_i)$ , with  $i = 1, 2$  and  $i \neq j$  denote the two particles. The shear rate  $\dot{\gamma}$  defines the Weissenberg number  $Wi = \tau_0 \dot{\gamma}$ , in terms of the relaxation time  $\tau_0$  of the dumbbell in the absence of any flow. The noise vectors  $\xi_1$  and  $\xi_2$  are Gaussian random variables with correlation matrices:  $\langle \xi_i(t) \xi_j^T(t') \rangle = \delta_{ij} k_B T \eta(|t-t'|) \mathbf{I}_3$ , consistent with the fluctuation dissipation relation [18], where  $\mathbf{I}_3$  denotes the  $3 \times 3$  identity matrix. For the case of harmonically interacting dumbbells we choose  $V(|\mathbf{r}_i - \mathbf{r}_j|) = \frac{1}{2} \omega_0^2 (\mathbf{r}_i - \mathbf{r}_j)^2$ , which is a Rouse polymer of size  $N = 2$  [19].

The term inside the integral in Eq. (1) is the memory kernel representing a time-dependent friction. Consequently, the present state depends on the entire history. Physically, the GLE renders itself derivable in terms of mechanical equations for a particle interacting with a thermal bath, in terms of the spectral density of the bath oscillators [20, 21]. To address the problem at hand, we employ a power law decaying form for the memory kernel:  $\eta(t) = \eta_\alpha t^{-\alpha} / \Gamma(1 - \alpha)$ , with  $0 < \alpha < 1$  [22]. With this form of memory kernel, the GLE results in a subdiffusion for the motion of a free particle [23, 24].

*Center of mass motion for linear spring:* Absence of any external force on the dumbbell allows us to separate

\*rksinghmp@gmail.com

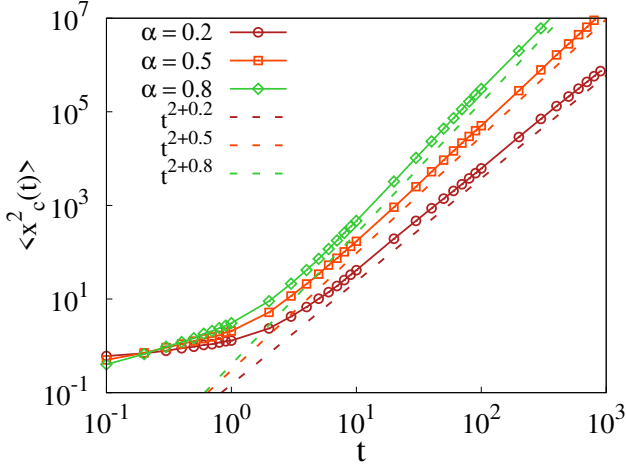


FIG. 1: Mean square displacement of the center of mass motion  $x_c$  along the shear flow direction for varying  $\alpha$ , with respective line fits. Parameter values for numerical calculation are:  $\dot{\gamma} = 1$ ,  $\eta_\alpha = 1$  and  $k_B T/2 = 1$ .

its dynamics into the motion of center of mass and motion about the center of mass. The coordinate of the center of mass  $\mathbf{r}_c = \frac{\mathbf{r}_1 + \mathbf{r}_2}{2}$  evolves as:

$$\int_0^t dt' \eta(t-t') (\dot{\mathbf{r}}_c - \dot{\gamma} y_c \mathbf{i})(t') = \xi_c(t), \quad (2)$$

where  $\xi_c(t) = [\xi_1(t) + \xi_2(t)]/2$  is Gaussian noise with mean zero and correlation:  $\langle \xi_c(t) \xi_c^T(t') \rangle = \frac{1}{2} k_B T \eta(|t-t'|) \mathbf{I}_3$ . It is evident looking at Eq. (2) that the center of mass moves like a free particle in shear flow. Interestingly, the  $y$  (and  $z$ ) components of motion do not feel the effect of shear flow, with the well known two-point correlation:  $\langle y(t_1) y(t_2) \rangle = k_B T / 2\eta_\alpha [t_1^\alpha + t_2^\alpha - |t_1 - t_2|^\alpha]$  [4]. The  $x$  component of motion is, however, affected by the presence of shear flow which is directed along the  $x$ -axis. Invoking the Laplace transform of Eq. (2) allows us to decouple the convolution of the memory kernel  $\eta$  and local velocity. As a result, the time evolution of the  $x$ -coordinate of the center of mass evolves as:

$$x_c(t) = \dot{\gamma} \int_0^t dt' y_c(t') + \int_0^t dt' g(t-t') \xi_{cx}(t'), \quad (3)$$

where  $\tilde{g}(s) = 1/s\tilde{\eta}(s)$ , is the Laplace transform of  $g$ . This allows us to address the effect of shear flow on center of mass motion, which in terms of mean square displacement reads:

$$\begin{aligned} \langle x_c^2(t) \rangle &= \frac{\dot{\gamma}^2 k_B T}{\eta_\alpha} \frac{\alpha + 1}{\Gamma(\alpha + 3)} t^{\alpha+2} + \frac{k_B T}{\eta_\alpha} \frac{t^\alpha}{\Gamma(\alpha + 1)}, \\ &\approx \frac{\dot{\gamma}^2 k_B T}{\eta_\alpha} \frac{\alpha + 1}{\Gamma(\alpha + 3)} t^{\alpha+2}, \end{aligned} \quad (4)$$

with the shear contribution dominating at large times. This is an interesting result, in that motion along the flow is shear dominated and thermal fluctuations play only a

sub-dominant role. It also generalizes the earlier study on viscous shear flows ( $\alpha = 1$ ):  $\langle x_c^2(t) \rangle = \frac{2}{3} \dot{\gamma}^2 D t^3$  [25], with  $D = k_B T / 2\eta_\alpha$ . Numerical solution of Eq. (2) provides a confirmation of our analytical results [26, 27] (cf. Fig. 1). The subdiffusive nature of motion at small times viz.  $t \lesssim 1$  is also discernible from Fig. 1. This implies that the shear flow results in a crossover from subdiffusive motion to a motion faster than ballistic.

*Relative motion for linear spring:* The relative coordinate  $\mathbf{r}_r = \mathbf{r}_1 - \mathbf{r}_2$  evolves as:

$$\int_0^t dt' \eta(t-t') (\dot{\mathbf{r}}_r - \dot{\gamma} y_r \mathbf{i})(t') = -2\omega_0^2 \mathbf{r}_r + \xi_r(t), \quad (5)$$

and represents a particle moving in a harmonic potential in a viscoelastic medium under shear. The noise variable  $\xi_r(t) = \xi_1(t) - \xi_2(t)$  is an unbiased colored Gaussian noise with correlation matrix  $\langle \xi_r(t) \xi_r^T(t') \rangle = 2k_B T \eta(|t-t'|) \mathbf{I}_3$ .

As the  $y$  (and  $z$ ) component does not feel the effect of flow, its dynamics is known exactly:  $\langle y_r(t) y_r(t') \rangle = 2k_B T [Q(t) + Q(t') - 2\omega_0^2 Q(t)Q(t') - Q(|t-t'|)]$  [28, 29], where  $Q(t) = \frac{1}{2\omega_0^2} [1 - E_\alpha(-at^\alpha)]$  [30] where  $a = \frac{2\omega_0^2}{\eta_\alpha}$  and  $E_\alpha(\cdot)$  is the Mittag-Leffler function [31]. The motion along  $x$  direction, however, feels the effect of both thermal fluctuations and shear flow, with the former known exactly. The shear contribution to the motion in Laplace domain reads:  $\tilde{x}_r(s)_{Sh} = \dot{\gamma} \tilde{G}(s) \tilde{y}_r(s)$  with  $\tilde{G}(s) = \frac{s^{\alpha-1}}{s^\alpha + a}$ , and allows us to calculate the fluctuations in the relative coordinate:  $\frac{\langle x_r^2(t) \rangle_{Sh}}{\dot{\gamma}^2} = \int_0^t dt_1 G(t-t_1) \int_0^t dt_2 G(t-t_2) \langle y_r(t_1) y_r(t_2) \rangle$ . Now, using the 2-point correlation of  $y$  and using the following integrals:  $\int_0^t dt_1 G(t-t_1) = t E_{\alpha,2}(-at^\alpha)$ ,  $\int_0^t dt_1 G(t-t_1) Q(t_1) = (G * Q)(t) = R(t) = \frac{at^{\alpha+1}}{2\omega_0^2} E_{\alpha,2}^{(1)}(-at^\alpha)$  and  $\int_0^t dt_1 G(t-t_1) \int_0^t dt_2 G(t-t_2) Q(|t_1-t_2|) = 2 \int_0^t dt_1 G(t_1) R(t_1)$ , we have:

$$\begin{aligned} \frac{\langle x_r^2(t) \rangle_{Sh}}{2\dot{\gamma}^2 k_B T} &= \frac{t^2}{\omega_0^2} \sum_0^\infty \sum_0^\infty \frac{l(-at^\alpha)^{k+l}}{\Gamma(\alpha k + 1) \Gamma(\alpha l + 2) [\alpha(k+l) + 2]} \\ &+ \frac{t^2}{2\omega_0^2} [2at^\alpha E_{\alpha,2}(-at^\alpha) E_{\alpha,2}^{(1)}(-at^\alpha) - a^2 t^{2\alpha} \{E_{\alpha,2}^{(1)}(-at^\alpha)\}^2], \end{aligned} \quad (6)$$

where  $E_{\alpha,\beta}(\cdot)$  is the two-parameter Mittag-Leffler function and  $E_{\alpha,\beta}^{(1)}(\cdot)$  its derivative [31]. Let us make an approximation, viz.  $\frac{l}{\alpha(k+l)+2} \approx \frac{l}{2}$ , which is expected to hold for small values of  $\alpha$ , for the first term in Eq. (6) and the asymptotic forms of  $E$  and  $E^{(1)}$  [32] in the second term, we have:

$$\langle x_r^2(t) \rangle_{Sh} \sim \frac{\alpha \dot{\gamma}^2 k_B T}{a^2 \omega_0^2 \Gamma^2(2-\alpha)} t^{2-2\alpha}. \quad (7)$$

This implies that the shear contribution to the motion of the relative coordinate grows without bounds, in a superdiffusive manner ( $\alpha$  is small). In addition, as the

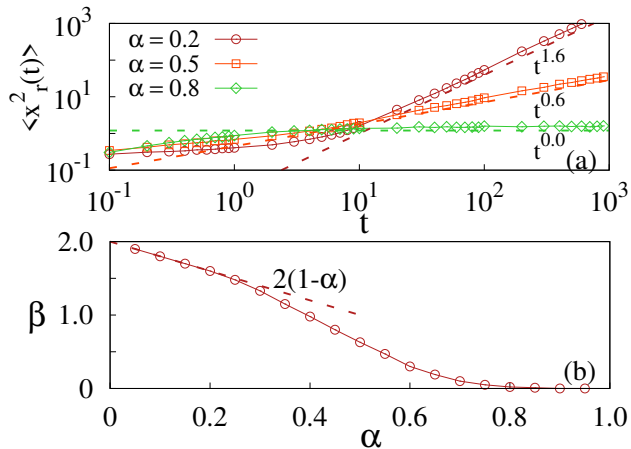


FIG. 2: (a) Mean square displacement of the relative motion  $x_r$  along the shear flow direction for various  $\alpha$ , with respective line fits. (b) Dependence of  $\beta$  on the exponent of subdiffusion  $\alpha$ . Parameters for the numerical calculation are:  $\dot{\gamma} = 1$ ,  $\eta_\alpha = 1$ ,  $2k_B T = 1$  and  $\omega_0 = 1$ .

thermal contribution eventually reaches a steady value, this is the fate of separation between the two masses in that  $\langle x_r^2(t) \rangle \sim t^\beta$  with  $\beta = 2(1 - \alpha)$  (for small  $\alpha$ ). For arbitrary values of  $\alpha$ , such a closed form expression is not possible, and we solve Eq. (5) numerically to assess the behavior of fluctuations in the separation of the two masses. We show the results for  $\langle x_r^2(t) \rangle$  in Fig. 2(a) for different values of  $\alpha$ . For the entire range of  $\alpha \in (0, 1)$ , Fig. 2(b) shows that the fluctuations in the relative coordinate go from superdiffusive to diffusive to subdiffusive as  $\alpha$  grows from 0 to 1[26]. The deviation from the straight line behavior is also evident, implying towards the failure of the approximation made to decouple the series in Eq. (6).

Nonexistence of the steady-state for the motion of relative coordinates implies that the system does not feel the effects of confinement. Hence, the harmonically interacting dumbbell which serves as a starting point for addressing tumbling in viscous shear flows, *e.g.*- Rouse chains [33, 34], does not work for motion in viscoelastic medium under shear. As a result, we need a potential strong enough to exhibit a nonequilibrium steady state for the motion of relative coordinates. In the next section, we address this problem by introducing nonlinear interactions and study tumbling of dumbbells in viscoelastic shear flows.

*Generalized Langevin equation in shear flows-Nonlinear dumbbell model:* In order to bring in nonlinearity in the problem, we introduce FENE-LJ potential which is more realistic compared to the harmonic interaction [16]. The inter-particle interaction is a contribution from both repulsive and attractive parts,

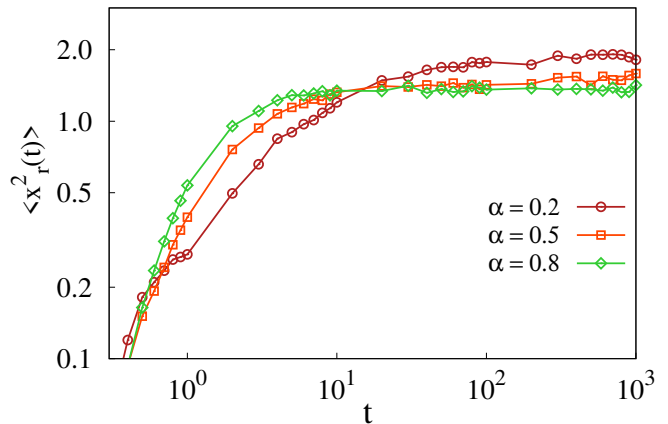


FIG. 3: Mean square displacement of relative separation  $x_r$  of two particle connected by a nonlinear spring for different values of  $\alpha$ .

viz.  $V = V_{LJ} + V_{FENE}$ , wherein

$$V_{LJ}(r) = 4\varepsilon[(\sigma/r)^{12} - (\sigma/r)^6], \text{ and} \quad (8a)$$

$$V_{FENE}(r) = -(kR_0^2/2) \ln[1 - (r/R_0)^2]. \quad (8b)$$

As mentioned earlier, we consider only the repulsive part of  $V_{LJ}$ . In above equations,  $r = |\mathbf{r}_1 - \mathbf{r}_2|$  denotes the separation between the two monomers,  $\sigma$  their size,  $\varepsilon$  the strength of repulsion,  $R_0$  the maximum extension, and  $k$  the stiffness constant. The force on particle  $i$  due to  $j$  is  $-\nabla_i V(|\mathbf{r}_i - \mathbf{r}_j|)$ , with  $i, j = 1, 2$ . The resulting equations of motion read:

$$\begin{aligned} \ddot{\mathbf{r}}_i + \int_0^t dt' \eta(t-t') (\dot{\mathbf{r}}_i - \dot{\gamma} y_i \mathbf{i})(t') \\ = -\nabla_i V(|\mathbf{r}_i - \mathbf{r}_j|) + \dot{\gamma} y_i \mathbf{i} + \xi_i(t), \end{aligned} \quad (9)$$

with  $i, j = 1, 2$  and  $i \neq j$ . We have retained the acceleration terms for the nonlinear system because of its numerical advantage (avoids root finding like in the overdamped case) [26]. The second term on the right hand side of the above equations,  $\dot{\gamma} y_i$  is the coordinate dependent contribution from the flow. This term arises when we take account of the local streaming velocity alongwith the actual momentum [25]. Similar to the case of overdamped motion, the center of mass for underdamped motion also follows  $\langle x_c^2(t) \rangle \sim t^{\alpha+2}$ . The nonlinear spring, however, unlike the harmonic spring, achieves a steady-state owing the FENE-LJ potential which keeps the bond-length in the interval  $(\sigma, R_0)$ . This is evident from the behavior of the mean square displacement  $\langle x_r^2(t) \rangle$  of the relative separation between the two masses connected by the nonlinear spring (*cf.* Fig. 3).

In what follows, energy is measured in units of  $\varepsilon$  and distance in units of  $\sigma$ . In addition, following [35, 36], we choose:  $\varepsilon = 1$ ,  $\sigma = 1$ ,  $R_0 = 1.5\sigma$ ,  $k = 30\varepsilon/\sigma^2$ ,  $k_B T = 1.2\varepsilon$  and  $\eta_\alpha = 7.5$ .

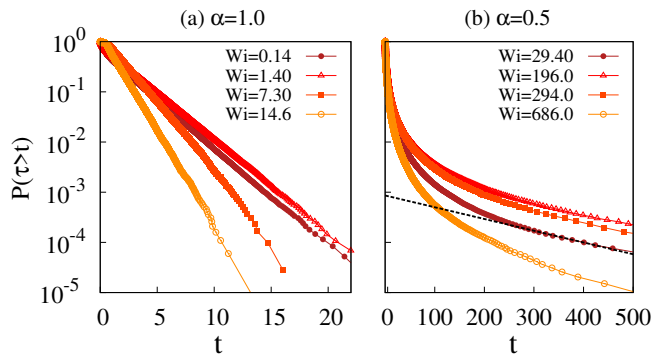


FIG. 4: Probability distribution  $P(\tau \geq t)$  for the dumbbells tumbling in (a) purely viscous shear flow ( $\alpha = 1$ ) vs (b) viscoelastic shear flows ( $\alpha = 0.5$ ). The exponentially decaying tails for the two cases are discernible from the graphs (line fit for  $Wi = 29.40$ ), with the distributions of the form  $P(\tau \geq t) \approx \exp(-\nu\tau)$ . In addition, a change in the trend of slope for the two types of flows is also clearly evident.

*Distribution of tumbling times:* Tumbling time  $\tau$  is defined as the interval of successive zero-crossings of the end-to-end vector  $R_x = x_1 - x_2$ . The distribution of tumbling times  $P(\tau \geq t)$  in purely viscous flow exhibits exponentially decaying tails for various values of the Weissenberg number  $Wi$  (Fig. 4 (a)). Interestingly, even for tumbling in viscoelastic shear flow,  $P(\tau \geq t)$  exhibits exponentially decaying tails (*cf.* Fig. 4 (b)), though the time  $\tau$  taken for the viscoelastic case is much longer when compared to its viscous counterpart. In addition, the tumbling events for the two types of flows, *viz.* viscous and viscoelastic case occur at different levels of flow strengths. As a matter of fact, the observed values of flow strength for the viscoelastic case are well beyond the experimentally observed ranges for the case of viscous shear flows. This is evident from the respective values of  $Wi$  for the two cases, which are at least an order of magnitude apart. The reason for this difference is that relaxation time in a viscoelastic medium is much longer compared to relaxation in a purely viscous fluid. In other words, the effect of viscoelasticity in the medium is to slow down the characteristic tumbling frequency at finite  $Wi$  consistent with earlier studies [37–39] for rotational dynamics of suspended particle in viscoelastic shear flow. The exponentially decaying tails of the tumbling time distribution,  $P(\tau \geq t) \approx \exp(-\nu\tau)$ , define the characteristic tumbling time  $\tau_{tumb}$  as inverse of the characteristic exponent  $\nu$ . In addition, for the case of purely viscous flows, *i.e.* for  $\alpha = 1$ , we find via numerical calculations that  $\nu\tau_0 \approx Wi^{0.67}$  for  $Wi \gg 1$  [40], wherein  $\tau_0$  is relaxation time of the autocorrelation  $\langle R_x(t)R_x(t+T) \rangle$ .

*Effect of subdiffusion on tumbling:* We study the effect of subdiffusion on tumbling of dumbbells in Fig. 5, wherein we find that  $\nu\tau_0$  exhibits a nonmonotonic behavior with  $Wi$  which is absent in viscous medium (*cf.* inset of Fig. 5). Though there is a slight deviation in the

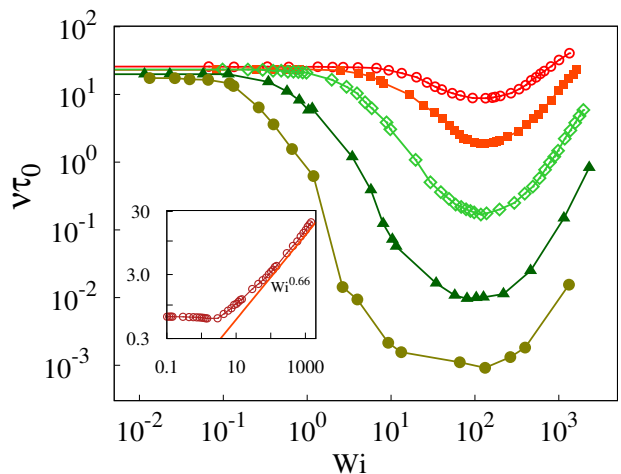


FIG. 5: Limiting decay rate  $\nu$  scaled with  $\tau_0$  vs  $Wi$  for subdiffusive case for different values of  $\alpha$ . For weak flow strengths, *i.e.* for  $Wi \ll 1$ , the different curves trace each other. On the other hand, for  $Wi \gg 1$ , the  $\nu\tau_0$  grows with the Weissenberg number as  $Wi^{\mu(\alpha)}$ , where the exponent  $\mu$  depends on  $\alpha$ . Inset shows the variation of dimensionless tumbling frequency  $\nu\tau_0$  with the Weissenberg number  $Wi$  for a dumbbell tumbling in a purely viscous medium ( $\alpha = 1$ ).

trends of the curve for distribution with increasing  $Wi$  (*cf.* Fig. 4 (a) for  $\alpha = 1$ ) showing nonmonotonicity in value of  $\nu$  but it is negligible compared to the case for  $\alpha < 1$ . To understand this behavior of  $\nu\tau_0$  vs  $Wi$ , let us have a look at Eq. (9), from where it is clear that the relative coordinate  $\mathbf{r}_1 - \mathbf{r}_2$  follows the motion of a single particle in the potential  $V = V_{FENE} + V_{LJ}$ , and in the absence of shear relaxes at its natural time scale dictated by the parameters of the potential and the degree of subdiffusion  $\alpha$ . However, when a small but finite amount of shear flow is introduced, it tends to align the dumbbell along the flow. With an increase in the strength of flow, a feedback from the elastic force which tends to preserve the previous relaxation, results in an enhanced tumbling time. Thus, resulting in a decrease in the tumbling frequency  $\nu\tau_0$  for small  $Wi$ . On the other hand, for strong flow, when  $Wi$  is quite large, tumbling occurs more frequently due to the increase in the rotational component of shear force dominating the tumbling dynamics. Consequently, for some intermediate value of  $Wi$ , the tumbling frequency  $\nu\tau_0$  hits a minima and our numerical calculations also corroborate this fact.

We also learn from Fig. 5 that the tumbling time  $\nu\tau_0$  changes significantly at any given value of  $Wi$  even for slight decrease in the value of  $\alpha$ . This is because the fluctuations in the relative coordinate are reduced for low values of  $\alpha$ , thus making tumbling a flow dominant phenomena which tends to keep the dumbbell oriented along the flow, hence the increase in tumbling time. Interestingly, for viscoelastic case, the increase in  $\nu$  starts at quite a high value of  $Wi$  as compared to the viscous case. This shift is consequent of the prolonged relaxation

in viscoelastic medium due to inherent elasticity.

Now, in the limit of very large values of the Weissenberg number, *i.e.*- for  $Wi \gtrsim 100$  for which  $\nu\tau_0$  is observed to monotonically increase with  $Wi$  with exponent close to 0.67 ( $\alpha = 1$ ) as  $\alpha$  approaches unity. However, for arbitrary values of  $\alpha$  we have not been able to extract reliable statistics of tumbling times so as to furnish a value of the growth exponent defining the scaling behavior:  $\nu\tau_0 \approx Wi^{\mu(\alpha)}$  [26]. This is because with decreasing  $\alpha$ , a tumbling event becomes rare to observe making it computationally very challenging to record them in a finite amount of computational time available to us.

*Conclusion:* Viscoelasticity is more of a rule rather than exception, and motivated by this, we have studied in this paper the transport and tumbling properties of polymers in a viscoelastic fluid under shear. Using dumbbells as representative, we provide analytical results for the motion of center of mass and separation between the two masses. For the simplest case of a harmonic spring connecting the two masses, we that the mean square displacement of the center of mass follows:  $\langle x_c^2(t) \rangle \sim \dot{\gamma}^2 t^{\alpha+2}$ ,  $0 < \alpha < 1$ , generalizing the earlier result:  $\langle x_c^2(t) \rangle \sim \dot{\gamma}^2 t^3$  ( $\alpha = 1$ ). On the other hand, fluctuations in the relative coordinate also grow monotonically

with time, with  $\langle x_r^2(t) \rangle \sim t^\beta$ , where  $\beta = 2(1 - \alpha)$  up to  $\alpha \approx 0.25$  and approaches 0 as  $\alpha$  approaches unity. Consequently, the system of two masses connected by a harmonic spring does not achieve a steady-state. In other words, the extensively studied Rouse polymer is inappropriate to address the dynamics of polymers in viscoelastic medium under shear. We remedy this pathology by introducing a nonlinear spring in the form of FENE-LJ interaction which restricts the separation of the two masses to a maximum allowed limit. Employing the nonlinearity in the system we address tumbling of dumbbells and find that the effect of viscoelasticity in medium is to slow down the characteristic tumbling frequency at finite  $Wi$ . We hope that our work motivates further studies along this direction, particularly the effect of hydrodynamic interactions on tumbling aspects.

### Acknowledgments

We thank Dibyendu Das for insightful discussions. SS and SK also acknowledge the financial assistance from SERB and INSPIRE program of DST, New Delhi, India.

- 
- [1] J. C. Maxwell, *Philos. Trans. R. Soc. Lond.* **157**, 49 (1867).
  - [2] R. S. Lakes, *Viscoelastic Solids* (CRC Press, Boca Raton, 1999).
  - [3] R. A. L. Jones, *Soft Condensed Matter* (Oxford University Press, Oxford, 2002).
  - [4] J.-H. Jeon and R. Metzler, *Phys. Rev. E* **81**, 021103 (2010).
  - [5] B. B. Mandelbrot and J. W. van Ness, *SIAM Rev.* **10**, 422 (1968).
  - [6] J. Szymanski and M. Weiss, *Phys. Rev. Lett.* **103**, 038102 (2009).
  - [7] S. C. Weber, A. J. Spakowitz, and J. A. Theriot, *Phys. Rev. Lett.* **104**, 238102 (2010).
  - [8] I. Bronstein, Y. Israel, E. Kepten, S. Mai, Y. Shav-Tal, E. Barkai, and Y. Garini, *Phys. Rev. Lett.* **103**, 018102 (2009).
  - [9] D. E. Smith, H. P. Babcock, and S. Chu, *Science*, **283** 1724 (1999); and references therein.
  - [10] P. LeDuc, C. Haber, G. Bao, and D. Wirtz, *Nature* **399**, 564 (1999).
  - [11] F. B. Usabiaga and R. Delgado-Buscacioni, *Macromol. Theory Simul.* **20**, 466 (2011).
  - [12] C. M. Schroeder, R. E. Teixeira, E. S. G. Shaqfeh, and S. Chu, *Phys. Rev. Lett.* **95**, 018301 (2005).
  - [13] R. G. Winkler, *Phys. Rev. Lett.* **97**, 128301 (2006).
  - [14] N. Özkaya and M. Nordin, *Fundamentals of Biomechanics* pp. 195-218, Springer, New York (1999).
  - [15] M. Herrchen and H. C. Öttinger, *J. Non-Newtonian Fluid Mech.* **68**, 17 (1997).
  - [16] K. Kremer and G. S. Grest, *J. Chem. Phys.* **92**, 5057 (1990).
  - [17] R. Zwanzig, *J. Stat. Phys.* **9**, 215 (1973).
  - [18] R. Kubo, *Rep. Prog. Phys.* **29**, 255 (1966).
  - [19] P. E. Rouse, *J. Chem. Phys.* **21**, 1272 (1953).
  - [20] U. Weiss, *Quantum Dissipative Systems*, 2nd ed. (World Scientific, Singapore, 1999).
  - [21] R. Kupferman, *J. Stat. Phys.* **114**, 291 (2004).
  - [22] A. Gemant, *Phys.* **7**, 311 (1936).
  - [23] I. Goychuk, *Phys. Rev. E* **80**, 046125 (2009).
  - [24] K. G. Wang and M. Tokuyama, *Physica A* **265**, 341 (1999).
  - [25] M.G. McPhie, P.J. Daivis, I. K. Snook, J. Ennis and D.J. Evans, *Physica A* **299**, 412 (2001).
  - [26] See Supplementary Information details of the numerical calculations.
  - [27] I. Goychuk, *Adv. Chem. Phys.* **150**, 187 (2012).
  - [28] A. D. Viñales and M. A. Despósito, *Phys. Rev. E* **73**, 016111 (2006).
  - [29] M. A. Despósito and A. D. Viñales, *Phys. Rev. E* **77**, 031123 (2008).
  - [30] M. A. Despósito and A. D. Viñales, *Phys. Rev. E* **80**, 021111 (2009).
  - [31] I. Podlubny, *Fractional Differential Equations*, Academic Press (1999).
  - [32] J. R. Wang, Y. Zhou, and D. O'Regan, *Integral Transforms and Special Functions* **29**, 91 (2018).
  - [33] S. Bhattacharya, D. Das, and S. N. Majumdar, *Phys. Rev. E* **75**, 061122 (2007).
  - [34] D. Das and S. Sabhapandit, *Phys. Rev. Lett.* **101**, 188301 (2008).
  - [35] G.S. Grest and K. Kremer, *Phys. Rev. A* **33**, 3628 (1986).
  - [36] S. Singh and S. Kumar, *J. Chem. Phys.* **150**, 024906 (2019).
  - [37] G. D'Avino, N. A. Hulsen, K. Sijm, N. Vermant, O. Greco and P. L. Maffettone, *J. of Rheology* **52**, 1331

- (2008).
- [38] F. Snijkers, G. D'Avino, R. A. Maffettone, O. Greco, M. Hulsen and J. Vermant, *J. of Rheology* **53**, 459 (2009).
- [39] K. D. Housiadas and R. I. Tanner, *Phys. Fluids* **30**, 073101 (2018).
- [40] A. Celani, A. Puliafito and K. Turitsyn, *Europhys. Lett.*, **70**, 464 (2005).

# Supplementary Information for Tumbling dynamics of a dumbbell in viscoelastic shear flow

Sadhana Singh,<sup>1</sup> R. K. Singh,<sup>1,2,\*</sup> and Sanjay Kumar<sup>1</sup>

<sup>1</sup>*Department of Physics, Banaras Hindu University, Varanasi-221005*

<sup>2</sup>*Department of Physics, Indian Institute of Technology, Bombay, Powai, Mumbai-400076*

## I. EXTENSION TO POLYMERS

Let us generalize to the case of polymers in viscoelastic shear flow. We take a polymer of size  $N = 20$  with  $\alpha = 1/2$ . The equation of motion for the  $i$ -th monomer reads:

$$\ddot{\mathbf{r}}_i + \int_0^t dt' \eta(t-t') (\dot{\mathbf{r}}_i - \dot{\gamma} y_i \mathbf{i})(t') = - \sum_{j \neq i} \nabla_i V(|\mathbf{r}_i - \mathbf{r}_j|) + \dot{\gamma} y_i \mathbf{i} + \xi_i(t), \quad (1)$$

where  $V = V_{FENE} + V_{LJ}$  and  $\xi_i$  is an  $N$ -tuple of Gaussian random variables with power law correlation, with only the repulsive part of the LJ potential (athermal good solvent conditions) employed to address excluded volume effect amongst non-bonded beads.

Even though the polymer is an extended object composed of  $N$  monomers, its center of mass  $\mathbf{r}_c = \sum_i \mathbf{r}_i / N$  moves like a free particle, with its mean square displacement  $\langle \mathbf{r}_c^2(t) \rangle \sim t^{\alpha+2}$ , as shown previously for dumbbells. The diffusion coefficient for the center of mass motion is, however, reduced by a factor of  $N$ . In order to calculate the tumbling time of the polymer for given value of Weissenberg number  $Wi$ , we numerically solve Eqns. (1) and calculate the zero-crossing times of the end-to-end vector  $x_1 - x_N$  along the shear flow. We find that for  $Wi \gg 1$ , the characteristic tumbling frequency  $\nu \tau_0 \sim Wi^\mu$  with  $\mu \approx 1.85 \pm 0.05$  for  $\alpha = 1/2$  (*cf.* Fig. 1), where  $\tau_0$  is the characteristic relaxation time of the autocorrelation of  $x_1 - x_N$  in the absence of shear. This compares well, for example, with the corresponding exponent for nonlinear dumbbells, for which  $\nu \tau_0 \approx Wi^{1.9}$  for  $\alpha = 1/2$ .

An important thing to notice about polymer tumbling is that the exponent characterizing tumbling in viscoelastic shear flow is identical in value (within errorbars) to the case of dumbbell. However, there is an important difference between the  $\nu \tau_0$  vs  $Wi$  graphs for the polymer as opposed to the dumbbell. It is evidently clear from Fig. 5 (main text) and Fig. 1 is that location of minima for polymer is about two orders of magnitude less than the corresponding value for dumbbells. This is consequent of the fact that a polymer, being an extended object, will exhibit a tumbling

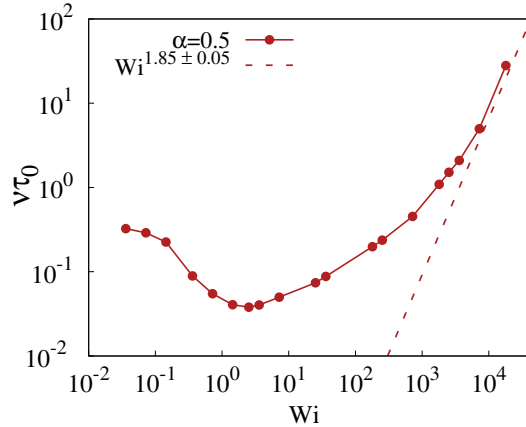


FIG. 1: Limiting behavior of the tumbling frequency  $\nu \tau_0$  with Weissenberg number  $Wi$  for a polymer of size  $N = 20$  for  $\alpha = 1/2$ . For  $Wi \gg 1$ , we find that  $\nu \tau_0 \sim Wi^{1.85 \pm 0.05}$ .

\*rksinghmp@gmail.com

event even in the extreme case when the two ends of polymer are close to each other (like in a U-shape). On the other hand, a dumbbell mostly remains as *extended* thus requiring more time to tumble.

In addition, as we have previously seen [1], polymers in a purely viscous medium do not exhibit a minima in the  $\nu\tau_0$  vs Wi curve, in a good solvent. However, exhibition of a minima for a polymer tumbling in a viscoelastic shear flow implies that the elastic component of the background fluid tends to slow down the occurrence of tumbling. At high shear rates, however, the behavior is similar to motion in viscous media.

## II. EMBEDDING FOR OVERDAMPED MOTION IN SHEAR FLOW

For simplicity, we discuss the concept for a single particle moving in the  $x-y$  plane in a viscoelastic fluid experiencing shear along the  $x$ -axis. The generalized Langevin equation describing the overdamped dynamics reads:

$$\int_0^t dt' \eta(t-t') (\dot{x} - \dot{\gamma}y)(t') = -V'_x(x, y) + \xi_x(t), \quad (2a)$$

$$\int_0^t dt' \eta(t-t') \dot{y}(t') = -V'_y(x, y) + \xi_y(t), \quad (2b)$$

where  $\xi_{x,y}(t)$  are Gaussian random variables with correlations

$$\langle \xi_x(t) \xi_y(t') \rangle = \delta_{xy} k_B T \eta(|t-t'|). \quad (3)$$

The friction kernel is a power-law decaying function of time:  $\eta(t) = \eta_\alpha t^{-\alpha} / \Gamma(1-\alpha)$  with  $0 < \alpha < 1$ . In order to solve Eq. (6), we employ the technique of Markovian embedding. We follow the review by Goychuk [2] and outline the methodology here for motion in shear flow. As only the  $x$  coordinate involves a contribution from shear flow, we focus only on motion along  $x$ -direction. Define  $u_i = -k_i(x - \dot{\gamma} \int_0^t dt' y(t') - x_i)$ , where  $x_i$  are auxiliary variables following

$$\eta_i \dot{x}_i = k_i u_i + \sqrt{2\eta_i k_B T} \xi_i(t), \quad (4)$$

with  $k_i = C_\alpha(b) \eta_\alpha \nu_0^\alpha / [b^{\alpha(i-1)} \Gamma(1-\alpha)]$  and  $\eta_i = C_\alpha(b) \eta_\alpha \nu_0^{\alpha-1} b^{(1-\alpha)(i-1)} / \Gamma(1-\alpha)$ , (*cf.* Eq. (23) in [2]). The numbers  $k_i$  and  $\eta_i$  define the Ornstein-Uhlenbeck processes

$$\dot{\zeta}_{i,x}(t) = -\nu_i \zeta_{i,x}(t) + \sqrt{2k_i \nu_i k_B T} \xi_{i,x}(t), \quad (5)$$

and are useful in approximating the power-law decay form with a sum of exponentials as  $\eta(t) = \sum_i k_i e^{-\nu_i t}$ , where  $\nu_i = k_i / \eta_i$ . The idea of representing power-law decay with such a form is fairly old [3]. The equivalence of Eq. (2) and (4) is easily shown, thus providing a way to numerically solve the former.

## III. MARKOVIAN EMBEDDING FOR UNDERDAMPED MOTION IN SHEAR FLOW

The generalized Langevin equation describing the dynamics of an underdamped particle in the  $x-y$  plane with a shear flow along  $x$ -axis reads:

$$\ddot{x} + \int_0^t dt' \eta(t-t') (\dot{x} - \dot{\gamma}y)(t') = -V'_x(x, y) + \dot{\gamma}y + \xi_x(t), \quad (6a)$$

$$\ddot{y} + \int_0^t dt' \eta(t-t') \dot{y}(t') = -V'_y(x, y) + \xi_y(t), \quad (6b)$$

where the symbols retain their usual meaning. The Markovian embedded form for the above equation in terms of auxiliary variables  $\{u_{i,x}\}_{i=1}^N$  and  $\{u_{i,y}\}_{i=1}^N$  is:

$$\dot{x} = v_x, \quad (7a)$$

$$\dot{v}_x = -V'_x(x, y) + \dot{\gamma}\dot{y} + \sum_{i=1}^N u_{i,x}(t), \quad (7b)$$

$$\dot{u}_{i,x} = -k_i(v_x - \dot{\gamma}y) - \nu_i u_{i,x} + \sqrt{2\nu_i k_i k_B T} \xi_{i,x}(t), \quad (7c)$$

$$\dot{y} = v_y, \quad (7d)$$

$$\dot{v}_y = -V'_y(x, y) + \sum_{i=1}^N u_{i,y}(t), \quad (7e)$$

$$\dot{u}_{i,y} = -k_i v_y - \nu_i u_{i,y} + \sqrt{2\nu_i k_i k_B T} \xi_{i,y}(t), \quad (7f)$$

where  $\xi_{i,x}$  and  $\xi_{i,y}$  are Gaussian white noise variables with mean zero and with correlations:  $\langle \xi_{i,x}(t) \xi_{j,y}(t') \rangle = \delta_{ij} \delta_{xy} \delta(t - t')$ . Now, from Eq. (A.3c) we have:

$$u_{i,x}(t) = - \int_0^t dt' (v_x - \dot{\gamma}y)(t') k_i e^{-\nu_i(t-t')} + \int_0^t dt' \sqrt{2\nu_i k_i k_B T} \xi_{i,x}(t') e^{-\nu_i(t-t')},$$

wherein we have used the initial conditions  $u_{i,x}(0) = 0$ . Substituting this in (A.3b) we have

$$\begin{aligned} \dot{v}_x &= -V'_x(x, y) + \dot{\gamma}\dot{y} - \int_0^t dt' (v_x - \dot{\gamma}y)(t') \sum_{i=1}^N k_i e^{-\nu_i(t-t')} + \sum_{i=1}^N \int_0^t dt' \sqrt{2\nu_i k_i k_B T} \xi_{i,x}(t') e^{-\nu_i(t-t')}, \\ &= -V'_x(x, y) + \dot{\gamma}\dot{y} - \int_0^t dt' (v_x - \dot{\gamma}y)(t') \eta(t-t') + \xi_x(t), \end{aligned}$$

where to obtain the last step we have used the solution of Eq. (A.4) and  $\xi_x(t) = \sum_i \zeta_{i,x}(t)$ . Similar calculations for the  $y$ -coordinate show the equivalence of Eq. (6) to the Markov embedded form (7). An important difference to be noted from the case of embedded form for overdamped motion is the absence of memory term for the underdamped dynamics.

It is noted that the representation of a power-law decaying function with a sum of exponentials serves a good approximation to the former only in a finite range  $[t_i, t_f]$ , beyond which there are exponential cutoffs. For all practical purposes, like the one considered here, the range  $[t_i, t_f]$  is sufficient. Following Ref. [2], we use an  $N = 16$  term exponential approximation for the power-law decaying memory kernel employing decade scaling  $b = 10$ . Also, the fastest time-scale  $\nu_0 = 10^3$ .

---

[1] S. Singh and S. Kumar, J. Chem. Phys. **150**, 024906 (2019).

[2] I. Goychuk, Adv. Chem. Phys. **150**, 187 (2012).

[3] R. G. Palmer, D. L. Stein, E. Abrahams, and P. W. Anderson, Phys. Rev. Lett. **53**, 958 (1984).